

DETECTION OF INTERLAMINAR CRACKS IN COMPOSITE STRUCTURES WITH THE USE OF PIEZOELECTRIC SENSORS AND THERMOGRAPHY

Piotr Kędziora

Cracow University of Technology
31-155 Kraków, ul. Warszawska 24, Poland
kedziora@mech.pk.edu.pl

Keywords: Delaminations, Thermography, Piezoelectric Sensors and Actuators, Lamb Wave, Composite Laminate.

Abstract. *Delaminations are one of the most severe defects associated with multilayered laminated composite structures. Initiation of delamination and numerical analysis of delamination growth are presented. Results of damage detection in composite laminated panels are demonstrated with use of piezoelectric patches and thermography. Thermography is utilized to detect and visualize the size of delaminations. Damage detection in fiber-reinforced composite laminated panels using Lamb waves (wave propagation) is demonstrated with the use of a sensor array. Experiments are conducted to empirically characterize the wave propagation behavior in a manufactured laminate. Piezoelectric patches are used as sensors and actuators in the experiments. Composite laminates are manufactured with an embedded defect to simulate inter-ply delamination.*

1 INTRODUCTION

Delaminations are one of the most severe defects associated with multilayered laminated composite structures. They may be caused by imperfections such as air entrapment and insufficient resin during fabrication or by impact and fatigue loads during services. Delaminations may lead to the severe degradation of the mechanical behavior of structures due to the loss of structural integrity. The detection of delaminations and the study of their effects on the mechanical behavior of delaminated composite structures become important practical issues.

Damage modeling in composite structures has been attempted by various researchers in the past. The latest effort includes a generalized laminate model featuring both weak interfacial bonding and local delamination by Shu [1]; a plasticity model coupled with the damage and identification for carbon fibre composite laminates by Boutaous et al. [2].

There have been many works on wave propagation problems related to composite shells. The first work (Lord-Rayleigh [3]) of this field dealt with wave propagation in a semi-infinite solid. In 1917 Lamb published the first work [4] of dealing with guided wave propagation in thin elastic specimens. Mirsky [5] and Nowinski [6] solved for axially symmetric waves in orthotropic shells. Chou and Achenbach [7] provided a three-dimensional solution for orthotropic shell as well. Nayfeh [8] discussed scattering of horizontally polarized elastic waves from multilayered anisotropic cylinders embedded in isotropic solids. Yuan and Hsieh [9] proposed an analytical method for the investigation of free harmonic wave propagation in laminated shells. The numerical description of the waves traveling into waveguides and slender structures has also raised many interests – information about those problems is discussed in Refs [10].

The first introduction of Lamb waves as a means of damage detection was made by Worlton [11] in 1961. He noticed that distinguish characteristics of the various modes of Lamb waves can be useful in nondestructive testing applications. Prosser et al. [12] used acoustic emission to identify cracking of thin composite specimens; also outlined the difficulties associated with acoustic emission. Wevers [13] outlined the advantages of acoustic emission techniques over other NDE methods for identifying damage in a loaded composite component. Lakshmanan and Pines [14] used and developed a wave propagation method to identify delaminations and transverse cracks in Gr/Ep composite rotorcraft. Ihn and Chang [15] used spectrograms to process guided wave signals obtained from an array of piezoelectric transducers to detect and monitor fatigue crack growth.

In this paper, we intend in order to assess the effect of delamination on the global characteristics of composite laminated cylindrical shells. Theoretical and numerical analysis of deformation initiation and growth is presented by Muc and Kędziora [16] and Muc [17]. Thermography is used to detect and visualize the size of delaminations. Results of damage detection in composite laminated panels are demonstrated with use of a piezoelectric sensor and thermography. Damage detection in fiber-reinforced composite laminated panels using Lamb waves (wave propagation) is demonstrated with the use of a sensor array. Experiments were conducted to empirically characterize the wave propagation behavior in a manufactured laminate. Piezoelectric patches were used as sensors and actuators in the experiments. Sensor arrays and associated processing were used for wave number decomposition and filtering of the Lamb wave modes. Composite laminates were manufactured with an embedded defect to simulate inter-ply delamination. Experiments were conducted to detect the presence of delamination damage in a composite laminate.

Comparisons were made between analytical predictions and experimental results, which demonstrate that the model captured essential wave propagation behavior at frequencies of interest.

2 INITIATION OF DELAMINATIONS – LINEAR FRACTURE MECHANICS

Using the continuum fracture (damage) mechanics concept it is possible to model fatigue phenomena taking into account macroscopic degradation models in the evaluation of an individual finite element (or group of them) mechanical properties – see e.g. Muc et al. [18]. However, in the distinction to the continuum fracture mechanics approach, the damage behavior of composites is represented here in the differential (incremental – not global, integral) form but in general, the method of the description is almost identical.

Employing formulations introduced in classical fracture mechanics several models for delamination growth in laminates may be proposed. Early experimental works point to strong correlation between the growth of cracks and the strain energy release rate G . The approximate size of delamination area A is governed by the following equation:

$$\frac{dA}{dN} = f(G_{\max}, \xi, \psi), \quad \xi = \frac{G_{\min}}{G_{\max}}, \quad \psi = a \tan\left(\frac{K_{II}}{K_I}\right) \quad (1)$$

where N is a number of cycles, and f denotes a function.

The parameter ξ expresses the ratio of minimum to maximum loading, and ψ denotes the relative amount of mode I (opening) and mode II (shearing). However, the mode dependence of the delamination growth is not yet fully understood and is a subject of considerable research.

For constant amplitude loading and a stable delamination growth, a power law relation has been first developed by Paris et al. [19]:

$$f(G_{\max}, \xi, \psi) = c(\Delta G)^n, \quad \Delta G = G_{\max} - G_{\min} \quad (2)$$

where c and n are material constants.

In the high stress intensity factor (SIF) range, the curve obtained from Eqs (1) and (2) is very steep indicating unstable crack propagation and hence the region does not contribute much to the propagation life of a component. Therefore, Forman et al. [20] improved the crack growth rate equation and proposed to apply the function f in the following form:

$$f(G_{\max}, \xi, \psi) = \frac{c(\Delta G)^n}{(1-R)K_c - \Delta G} \quad (3)$$

where R is the stress ratio, and K_c means the fracture toughness.

Since the delamination growth can be attributed to a mixed mode of fracture, the criterion for determining the initiation of the delamination growth was selected as [21]:

$$RB = g_1^\delta + g_2^\gamma, \quad g_1 = \frac{G_I}{G_{Ic}}, \quad g_2 = \frac{G_{II}}{G_{IIc}} \quad (4)$$

where RB is the failure index, G_{Ic} and G_{IIc} are the critical strain energy release rates corresponding to mode I and mode II fracture, respectively. δ and γ are coefficients – it was found that $\delta=\gamma=1$ provides the best fit to the experimental results (see [21]). A delamination would start to propagate when $RB \geq 1$.

3 NUMERICAL ANALYSIS OF DELAMINATION GROWTH

For instance let us consider the cross-ply laminate $[0^0, 90^0_n]_s$, loaded in a tension (equal to 1 MPa) along the x direction. The thickness of each individual ply is equal to t , so that the total thickness of the laminate is equal to $2(n+2)t$. The crack is described by its size a in the y direction and the position of its center x_a . The geometrical parameters of the laminate and of the crack are shown in Fig.1.

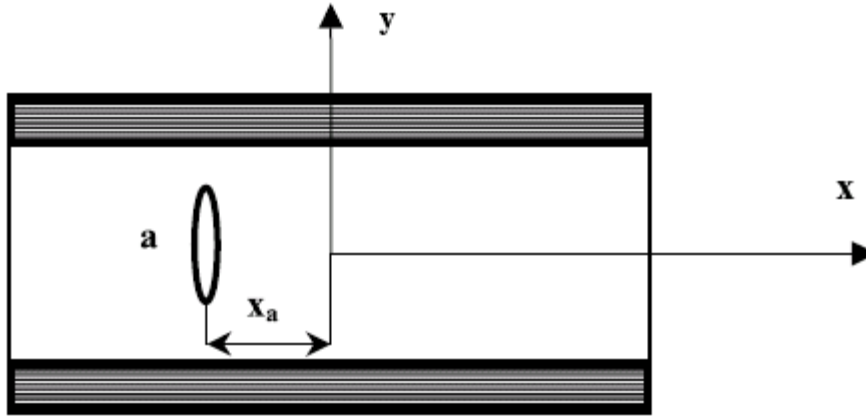


Figure 1: The geometrical parameters of the laminate with the crack.

The crack is always symmetric with respect to the x axis. Thus, only a half of the laminate is discretised with the use of finite elements. The plate have been modeled using 1536 2-D eight node isoparametric plane stress element. In the model crack face nodes are left free. The thickness of the laminate in the z direction is assumed to be equal to one. All geometrical quantities are given in mm.

With the aid of the presented finite element model the J-integral have been computed. In terms of stresses and strains it is defined as follows:

$$J = \int_{\Gamma} (Wn_1 - t_i u_{i,1}) ds \quad (5)$$

where W is the strain energy, u is displacement vector at any point on the contour, n_1 is the normal vector component, $u_{i,1}$ is the derivative of the displacement and t_i is the traction vector at the same point at the contour Γ . Γ is the contour starting from the crack face and going round the crack tip in an anti-clock wise direction and ending on the other crack face. This J-integral is seen to be the rate of change of potential energy with respect to the crack length a . For the linear elastic material the J-integral is equal to the energy release rate G . Since the laminate is subjected to the remote tension the first mode only is analyzed herein. In the evaluation of the J-integral, contour path is taken along the finite element edge and values and quantities in Eqn (5) are computed at the element level.

In the numerical analysis each ply is assumed to be made of carbon/epoxy resin having the following material properties (treated as it will be explained later as mean values): $E_1= 200$ [GPa], $E_2= 12$ [GPa], $G_{12}= 8$ [GPa], $G_{23}= G_{12}= 8$ [GPa], $G_{13}= 0.6 \cdot G_{12}= 4.8$ [GPa], $\nu_{12}= 0.3$. In order to verify the effectiveness of the proposed method of the numerical computations the analytical example dealing with the fracture analysis of a square isotropic homogeneous plate with central crack subjected to tension have been solved – see Broek [22]. Due to the central symmetry one quarter of the plate have been analyzed and discretised with the use of 768 finite elements. In the evaluation of the J-integral two contour paths are taken

to compare the results. Each contour paths runs around the crack tip from lower crack face up to the top crack surface along the finite element edges – it is drawn schematically in Fig. 2.

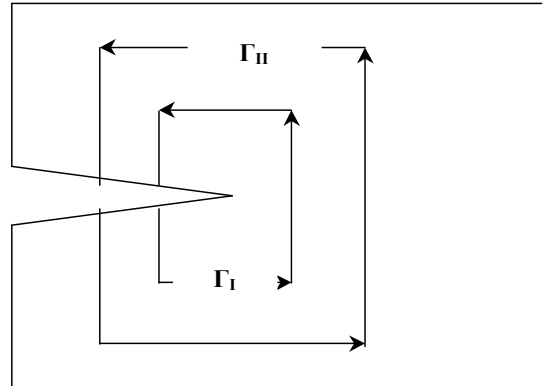


Figure 2: Contour paths Γ definitions.

The results of computations are presented in Table 1 together with the analytical results. The agreement between them seems to be very good. In further computations two different contour paths are always taken into considerations in order to eliminate possible errors in modeling of the path.

Path I	Path II	Analytical [22]
0.14374 E-04	0.15189 E-04	0.15122 E-04

Table 1: Comparison of analytical and numerical values of the J-integral.

4 EXPERIMENTAL ANALYSIS DAMAGE IDENTIFICATION

4.1 Detection of delamination via thermography

Thermography is a measurement technique which provides an image of the distribution of the temperature on the surface of the examined object. Thermography proceeds by decoding, using an adapted detector, information “temperature” resulting from the infra-red radiation emitted by any object. The principal advantage of infra-red thermography is its non-intrusive character. Indeed, it forms part of the techniques of non-destructive testing and can be carried out on installations in service. The deformation of solid materials is almost always accompanied by releases of heat. When the material becomes deformed or is damaged and fissured, a part of energy necessary to starting and the propagation of the damage is transformed in an irreversible way into heat [23].

During low frequency mechanical excitation, the average temperature in the gage section of the specimen increased with cycles. The small amplitude oscillatory temperature variation is due to the reversible thermal heating and cooling during each loading cycle. The objective in this study was to make a correlation between the increase in the temperature of specimen and the evolution of the damage [24].

The experimental analysis was conducted with the use of the thermovision camera Flir joined with the system IRNDT. The tested cylindrical panel was made of 8 layers and had the following geometrical parameters: $L=298$ [mm], $R=92$ [mm], $t=1.8$ [mm] – see Fig. 3. The thermal excitation was obtained from halogen lamps. During tests the temperature on the surface does not exceeded 40 [$^{\circ}\text{C}$] and the time of heating was equal to 20 [s].

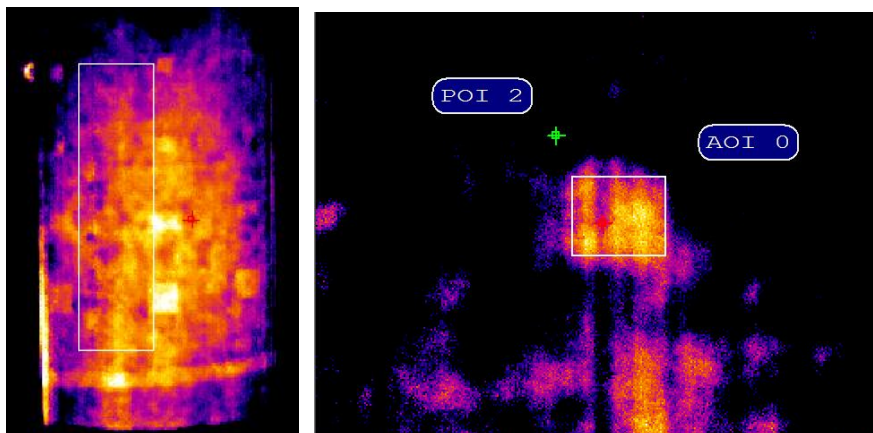
In the tested specimen delaminations were inserted at the shell mid-surface. They have different dimensions as it may be seen in Fig. 4. The plotted results demonstrate that the sensitivity of detection depends on the distance of the camera to the cylinder and on the lens diameter. It shows that those values have to be carefully chosen for each individual experimental case.



Figure 3: Experimented setup – an overview.

a) lens 18 [mm], distance 88 [cm]

b) lens 18 [mm], distance 16 [cm]



c) lens 10 [mm-], distance 30 [cm]

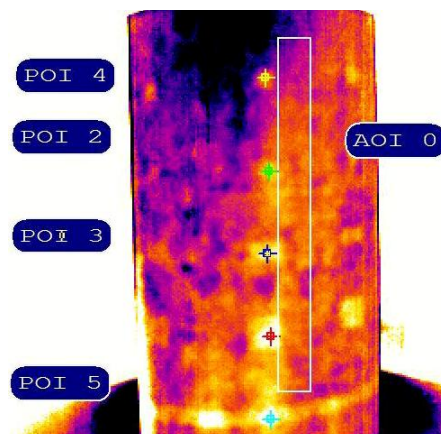


Figure 4: Effects of lens diameter and of distance to the specimen on the sensitivity of results.

Figure 5 represents the decrease of temperature with time for selected points at the panel. These values are particularly attributed to the location of delaminations.

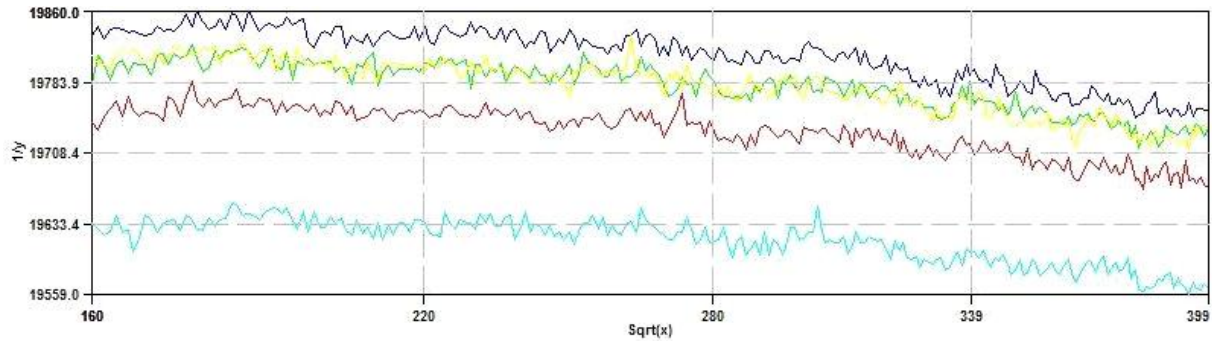


Figure 5: Graph of thermal response at selected locations.

4.2 Piezoelectric sensors

Damage detection in composite laminated panels using Lamb waves is demonstrated with use of a sensor array. Experiments were conducted to characterize empirically the wave propagation behavior in a manufactured laminate. Piezoelectric patches were used as sensors and actuators in the experiments. Sensor arrays and associated processing were used for wave number decomposition and filtering of the Lamb wave modes. Composite laminates were manufactured with an embedded defect to simulate inter-ply delamination. Experiments were conducted to detect the presence of delamination damage in a composite laminate.

A cylindrical panel made of glass woven roving having the mechanical and geometrical parameters identical to those mentioned in section 4.1 – Fig.6. An excitation signal took the form of sine wave function was modulated with the Hanning window and was applied at the left piezoelectric actuator in Fig.6; its frequency is varies from $100 \div 500$ [kHz]. The piezoelectric sensor (on the right side in Fig.6) was placed close to the local square delamination having the size 10 [mm] and being in the middle of the laminate.



Figure 6: General configuration of the cylindrical panel with one sensor and one actuator – they are located parallel to the delaminated area.

The wave propagation in the panel with local delamination was analyzed experimentally. The excitation signal and the response signal were generated and collected by the analyzer and then those signals were converted to digital ones with the use of MATLAB package.

Figure 7 demonstrates the response signals obtained experimentally for the perfect and imperfect (with the single delamination) cylindrical panel. As it may be seen there is a visible difference between response signals for perfect and imperfect shells for each excitation signal frequency considered.

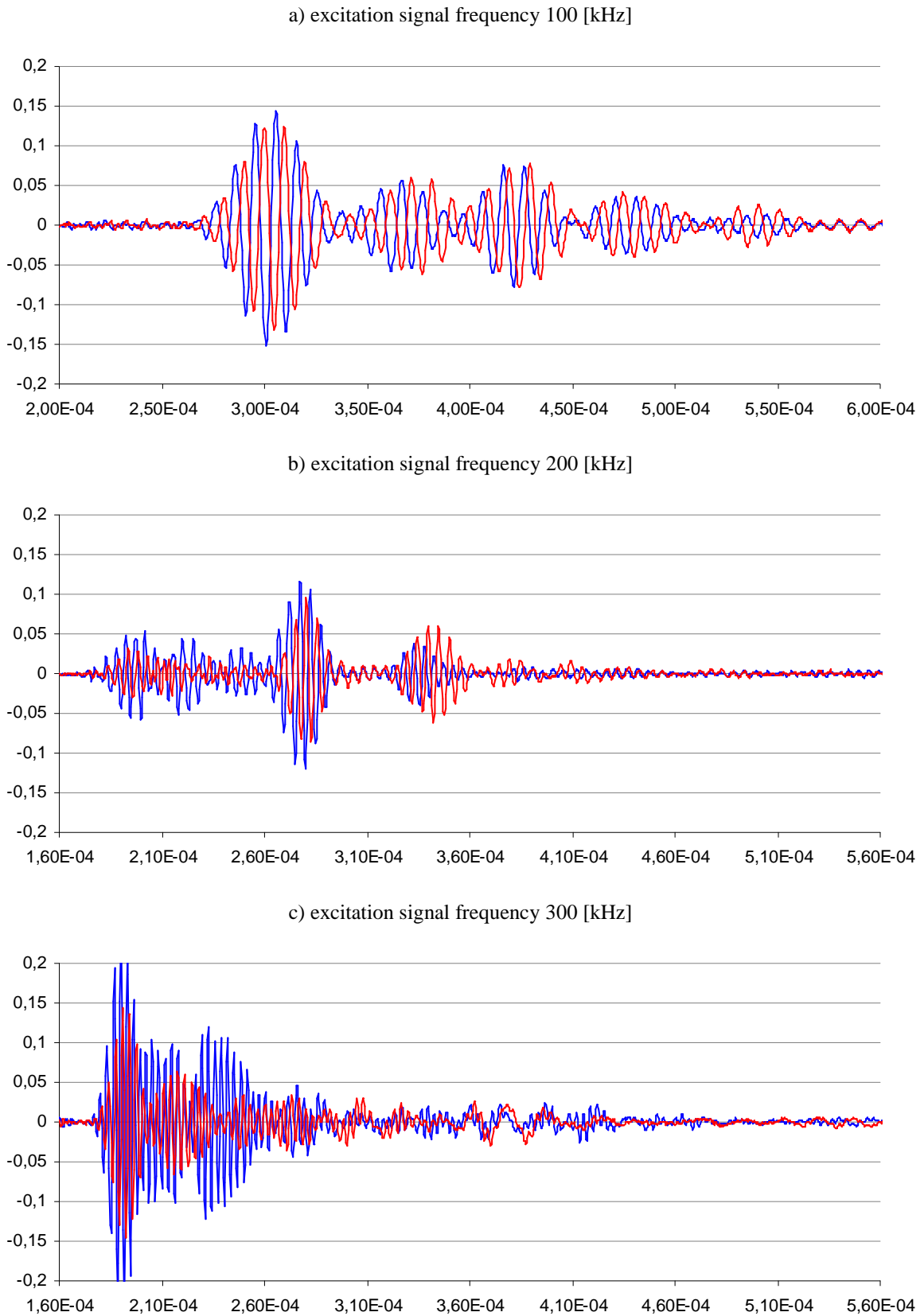


Figure 7: Experimental wave propagation results (blue line – without delamination, red line – with delamination); for various frequencies.

However, the reasonable detection of the size and the location of delamination require the careful analysis and optimal design of the location and number of piezoelectric sensors and actuator. In addition, in the delaminated region the interference between generated and reflected waves is observed that affects the signal collected by the sensor (see Figs 7a, b and c). In order to obtain better experimental results it is necessary to conduct further work dealing particularly with the optimal design of sensors number, locations and the frequency of the excitation signal.

The locations of piezoelectric sensor and actuator have significant effects on the displacement response. Different locations are presented in Figs 8 and 10. The response result (Figs 9 and 11) are plotted for one value of the signal excitation frequency equal to 100 [kHz]. The amplitude of response displacement is strongly affected by the distance between sensor and actuator – compare results plotted in Figs 7a and 11. The growth of the distance reduces the amplitudes. For the sensor and actuator located in the parallel direction to the delamination the amplitude for imperfect shell is lower than for perfect one, whereas for other locations the amplitude is higher – compare the results presented in Figs 7a and 9, 11.



Figure 8: Configuration of the cylindrical panel with the sensor and actuator – they are located below delaminated area 5 [cm] from the panel edge.

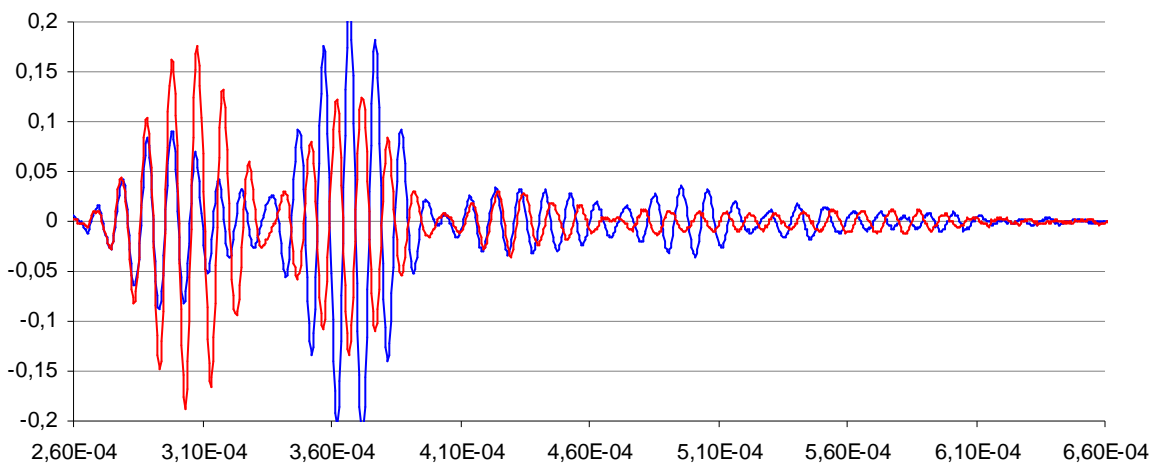


Figure 9: Experimental wave propagation results (blue line – without delamination, red line – with delamination); frequency is equal to 100 [kHz].



Figure 10: Configuration of the cylindrical panel with the sensor and actuator – the actuator is located above delaminated area 5 [cm] from the upper panel edge and the sensor 5 [cm] from lower panel edge.

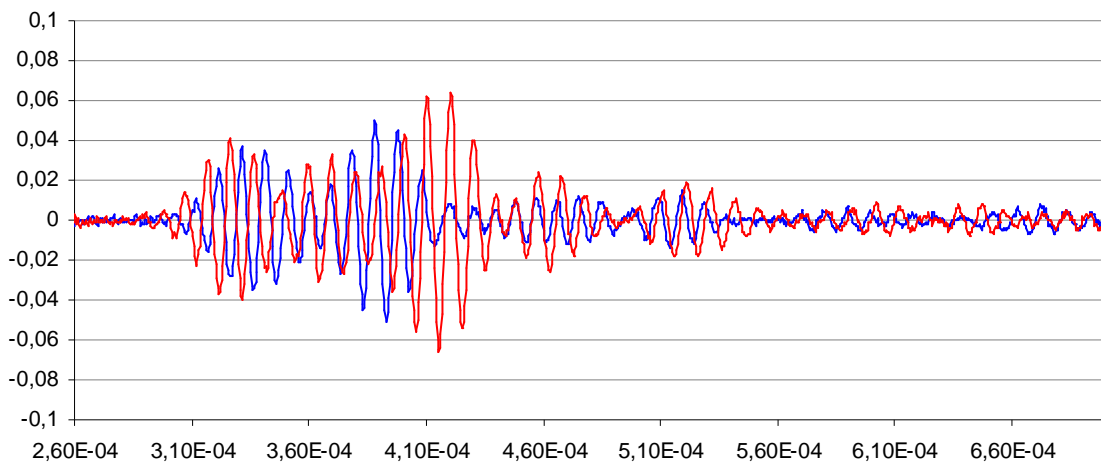


Figure 11: Experimental wave propagation results (blue line – without delamination, red line – with delamination); frequency is equal to 100 [kHz].

5 CONCLUSIONS

- This study is intended to show the relation between the dissipation of heat and the damage of the composites.
- These techniques propose to pass from temperature information given by the infrared camera to a distribution of heat sources on surface of the composites.
- The amplitude of the response is strongly affected by the excitation signal frequency and location of sensor and actuator; therefore, the optimization of they location and number is required.

ACKNOWLEDEGEMENT

The Polish Research Foundation PB 174/B/T02/2009/36 is gratefully acknowledged for financial support.

REFERENCES

- [1] X.P. Shu, A generalised model of laminated composite plates with interfacial damage. *Compos. Struct.*, **74**, 237-246, 2006.
- [2] A. Boutaous, B. Peseux, L. Gornet, A. Bélaidi. A new modeling of plasticity coupled with the damage and identification for carbon fibre composite laminates. *Compos. Struct.*, **74**, 1–9, 2006.
- [3] Lord-Rayleigh, On the Free Vibrations of an Infinite Plate of Homogeneous Isotropic Matter. *Proc. of the London Mathematical Society*, **20**, 225-234, 1889.
- [4] H. Lamb, On Waves in an Elastic Plate. *Proc. of the Royal Society*, London, **93**, 114–128, 1917.
- [5] I. Mirsky, Axisymmetric vibrations of orthotropic cylinders. *J. Acoust. Soc. Am.*, **36**, 2106, 1964.
- [6] J.L. Nowinski, Propagation of longitudinal waves in circular cylindrical orthotropic bars. *J. Engng. Ind.*, **89**, 408, 1967.
- [7] F.H. Chou, J.D. Achenbach, Three-dimensional vibrations of orthotropic cylinders. *ASCE J. Engng. Mech.*, **98**, 813, 1981.
- [8] A.H. Nayfeh, *Wave propagation in layered anisotropic media with applications to composites*. Elsevier, Amsterdam, 1995.
- [9] F.G. Yuan, C.C. Hsieh, Three-dimensional wave propagation in composite cylindrical shells, *Compos. Str.*, **42**, 153, 1998.
- [10] M.N. Ichchou, J.L. Mencik, W. Zhou, Wave finite elements for low and mid-frequency description of coupled structures with damage. *Comput. Methods Appl. Mech. Engrg.*, **198**, 1311, 2009.
- [11] D.C. Worlton, Experimental Confirmation of Lamb Waves at Megacycle Frequencies. *J. Appl. Ph.*, **32**, 967, 1961.
- [12] W.H. Prosser, K.E. Jackson, S. Kellas, B.T. Smith, J. McKeon, A. Friedman, Advanced, waveform based acoustic emission detection of matrix cracking in composites. *Materials Evaluation*, **53**, No. 9, 1052-1058, 1995.
- [13] M. Wevers, Listening to the sound of materials: acoustic emission for the analysis of material behavior. *NDT&E International*, **30**, No. 2, 99-106, 1997.
- [14] K.A. Lakshmanan, D.J. Pines, Modeling damage in rotorcraft flex beams using wave mechanics. *Smart Materials and Structures*, **6**, 383-392, 1997.
- [15] J.B. Ihn, F.K. Chang, Detection and monitoring of hidden fatigue crack growth using a built-in piezoelectric sensor/actuator network: I. Diagnostics. *Smart Materials and Structures*, **13**, 609-620, 2004.
- [16] A. Muc, P. Kędziora, A fuzzy set analysis for a fracture and fatigue damage response of composite materials. *Compos. Str.*, **54**, 283-287, 2001
- [17] A. Muc, A fuzzy set approach to interlaminar cracks simulation problems. *International Journal of Fatigue*, **24**, 419–427, 2002.
- [18] A. Muc, Z. Krawiec, FE modelling of laminates degradation in thin walled structures due to fatigue loads. *In: Proceedings WCCM-IV*, Buenos Aires, CD-Rom, I-588, 1998.

- [19] P.C. Paris, F. Erdogan, A critical analysis of crack propagation laws. *J. Basic Engng.*, Trans ASME, **85**, 528–534, 1963.
- [20] R.G. Forman, V.E. Keamey, R.M. Engle, Analysis of crack propagation in cyclic-loaded structures. *J. Basic Engng.*, Trans ASME, **87**, 459–464, 1967.
- [21] M.F. Kanninen, C.H. Popelar, *Advanced fracture mechanics*. Oxford engineering science series 15. Oxford University Press, 1985.
- [22] D. Broek, *Elementary engineering fracture mechanics*. Nijhoff, Hague, 1982.
- [23] A. Chrysochoos, Infrared thermography, a potential tool for analyzing the material behaviour. *Meca Indus*, **3**, 3-14, 2002.
- [24] L. Toubal, Analytical and experimental approaches of damage by fatigue of a carbon/epoxy composite. *Ph.D. thesis*, University Paul Sabatier, Toulouse III; 2004.